Journal of Fluorescence, Vol. 13, No. 1, January 2003 (© 2003)

Consequences of Inhomogeneous Broadening on Fluorescence Line Narrowing Spectra

A. D. Kaposi,[1,3] W. W. Wright,[2] and J. M. Vanderkooi[2]

Received July 6, 2002; accepted August 14, 2002.

Fluorescence line narrowing is a sensitive tool to monitor subtle changes in protein conformation. We restudied the consequences of inhomogeneous broadening on the observed spectra. Vibronic absorption bands of systems with weak electron-phonon coupling can be described by a lorentzian function with width of the order of a few centimeters. For an ensemble of molecules with closely spaced electronic transitions, a single laser frequency will excite many molecules through the broad base ("tail") of the lorentzian function. This, along with excitation of low-frequency modes, contributes to the unresolved background observed in line-narrowed spectra. Examples are shown for Zn cytochrome *c*, a fluorescent derivative of Fe cytochrome *c*. Spectra are compared for the protein in two solvents: glycerol/water or trehalose. Two types of cytochrome, from horse and yeast, are also compared.

KEY WORDS: Conformation; cytochrome *c*; porphyrin; trehalose.

INTRODUCTION

Heme proteins derive their color from the heme, but details of the hemoprotein absorption spectra reveal features of the polypeptide environment around the heme. In particular, the chromophore does not experience a unique environment, but there is a distribution of environments determined by the fluctuating positions of the neighboring amino acids and the intrinsic disorder of the protein. This results in inhomogeneous broadening of the optical transitions. Because fluctuations and disorder around hemes can affect their properties, the nature of the inhomogeneous broadening has been of especial interest for these proteins [1–4].

The specific issue we discuss in this paper is the effect of inhomogeneous broadening of the optical transitions on the emission spectrum. One consequence of inhomogeneous broadening is that, when excitation occurs into vibronic transitions that are closer spaced than the inhomogeneous distribution, a single excitation frequency can produce, in effect, more than one spectra that are shifted by the frequencies of the vibronic excited state [5]. This feature results in multiple 0,0 emission lines and produces resolved spectra with vibrational information on both the ground and excited state molecule. This is a powerful feature that allows the unambiguous identification of the compound, but there are also consequences of inhomogeneous broadening that reduce the resolution. The coupling of the chromophore with low-frequency modes of the surrounding matrix gives rise to phonon wings [5]. Because phonon wings (PWs) occur to the high-energy side of the optical transition, as one excites into the higher-frequency region of the inhomogeneous distribution, more and more molecules will be excited through the phonon wings, and the observed spectrum will have a larger contribution of the unresolved back-

[1] Department of Biophysics and Radiation Biology, Semmelweis University, Puskin u. 9, Budapest H-1088, Hungary.
[2] Johnson Research Foundation, Department of Biochemistry and Biophysics, University of Pennsylvania School of Medicine, Philadelphia, Pennsylvania 19104-6059.
[3] To whom correspondence should be addressed. Fax: +(36-1)-266-6656. E-mail kaposi@puskin.sote.hu

1053-0509/03/0100–0059/0

ground. We consider here another effect of the inhomogeneous broadening on the selection of molecules that are excited by a single laser frequency. This effect can be understood if one uses a model in which the inhomogeneous broadening is described by a distribution of energies (gaussian for perfect glass) but each absorption line is a lorenztian. The relaxation times from vibrationally excited states are on the order of 1 to 100 psec [6]. As expected from the uncertainty principle, a species that relaxes with a lifetime of 5 psec will have an absorption transition that can be described with a lorentzian function of width (FWHM) in the range of 1 cm^{-1}. A feature of lorentzian lines is that although they are narrow at the peak position, at the base they extend over a wide range. In a glassy system, there are many molecules that have slightly changed absorption. A single excitation frequency can excite many molecules through the extended lorentzian tails.

To consider effects of inhomogeneity, we use a long-lived excited state derivative of the hemoprotein cytochrome *c* (cyt *c*), where Zn is substituted for Fe. This derivative has nearly the same structure as native cyt *c* [7] but unlike Fe cyt *c*, the porphyrin of Zn cyt *c* is highly fluorescent. Under FLN conditions resolved spectra can be obtained, indicating that the overall absorption envelope is dominated by inhomogeneous broadening [8–10]. In an FLN experiment, one is able to distinguish 0,0 transitions from higher electronic and vibronic bands. The inhomogeneous distribution function (IDF), a measure of the distribution of 0,0 electronic transitions [11], broadens when the protein is denatured [12]. Molecular dynamics calculations indicate that fluctuation of the polypeptide chain is a contributing factor to the spectral inhomogeneous broadening, as is also indicated by sensitivity of the spectrum to the solvent glass transition. Spectra of porphyrins in protein and in solvents resemble each other, but in the protein the environment of the porphyrin can be changed with amino acid substitutions in a defined way. First, we compare cyt *c*'s from two different sources with known structure. In previous work it has been established that the *Q*(0,0) (i.e., alpha) band is split, attributed to asymmetry imposed by the polypeptide chain [13–15]. The splitting is less for the yeast protein, and the task is to separate the higher electronic band from the lower band. Second, we examine the effect of the solvent on the distribution of electronic origins. One solvent is glycerol/water with a glass transition of ~140 K, and this system is well known to preserve proteins at low temperature. The second is trehalose, which can form a glass at room temperature and above. Trehalose glass is of biological significance because a large number of species use this sugar as a cryoprotectant. It has been used to study the effect of solvent dynamics on proteins [16–18].

EXPERIMENTAL

Chemicals and Preparations

Trehalose, glycerol, and cyt *c* from horse and yeast were obtained from Sigma Chemical Co. (St. Louis, MO). Deionized, distilled water was used throughout.

Zn cyt *c* was prepared from the native protein as previously described [19]. To prepare the sample in glycerol/water (1:1 v/v) glass, the protein was simply dissolved in the solution. To prepare the protein in trehalose glass, the protein was dissolved in a 1:1 w/v trehalose/water solution, which was then plated onto a glass coverslip and the water was allowed to evaporate at 60°C. The resulting glass was hard to the touch. Independent infrared measurements revealed about 1–2 water molecules/trehalose molecule.

Spectroscopy

A Hitachi Perkin-Elmer absorption instrument was used to take the visible absorption spectra. The temperature was regulated using an OmniPlex cryostat (APD Cryogenics, Allentown, PA). A transmission cell holder with a 100-μm spacer was used for the glycerol solution. The thin spacer and the cryogenic co-solvent glycerol ensured that the sample remained optically clear at the low temperature. A Jobin-Yvon-Spex Fluorolog instrument (Edison, NJ) was used to obtain the conventional fluorescence spectra. The spectra were collected in the front-face mode. The same cryostat and cell holders were used as for the absorption measurements. Absorption and fluorescence spectra were sometimes again taken as the temperature warmed up to ascertain that no irreversible effects occurred. The concentration of protein used was 2–3 mM.

The FLN experiment used an instrument with a Coherent 899-01 ring dye laser pumped by an Innova 307 Ar ion laser (Coherent Laser Products, Palo Alto, CA). The dye used for excitation was Rhodamine 560 or 590 (Exciton Laser Dyes, Dayton, OH). The spectral width of the laser line was 0.5 cm^{-1}. The output to the sample was 0.3–0.6 mW/mm^2. Emitted light was obtained at 90° relative to excitation and collected in a THR 1000 monochromator (Jobin-Yvon, Longjumeau, France). Detection was with a cooled GaAs R943-02 PMT (Hamamatsu Photonics). The sample was maintained at 10 K with a closed cycle M22 cryostat (Cryophy-

sics SA, Geneva, Switzerland). The concentration of protein used was 100–200 μM.

Calculations

Simulations of spectra were carried out using Excel software (Microsoft) for the simulations with resolution of 10 and 1 cm^{-1} (21 and 201 data points in 200 cm^{-1} range). GCC (BeOS) software was used for simulations with the resolution of 0.01 cm^{-1} (20 001 data points in 200 cm^{-1} range).

RESULTS

Absorption, emission and FLN spectra of horse and yeast Zn cyt *c* at cryogenic temperature

The absorption of horse Zn cyt *c* is shown in Figure 1, along with the conventional fluorescence spectrum taken using broad-band excitation into the Soret peak. Two emission spectra, taken with laser excitation, are shown. The emission lines using excitation into the *Q*(0,1) band [(1,*m*)←(0,0) transition] shows sharp emission in the *Q*(0,0) region [(1,0)→(0,0) transition], as seen in Figure 1a$_1$. For Figure 1a, excitation was into the *Q*(0,0) region [(1,0)←(0,0) transition]. In this case, sharp emission in the *Q*(0,1) region [(1,0)→(0,*n*) transition]; reflected ground state vibrations.

In Figure 2, analogous spectra are shown for yeast Zn cyt *c*. One emission spectrum taken with laser excitation into the *Q*(0,1) band at cryogenic temperature is shown, along with the absorption and conventional fluorescence spectrum. The absorption spectrum does not show the vibronic fine-structure seen for the horse derivative (Fig. 1).

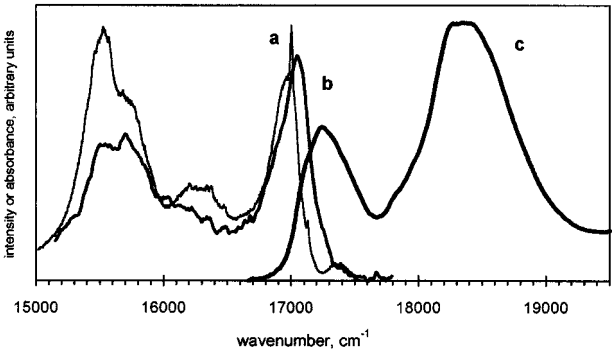

Fig. 2. Absorption (thick line, c), conventional fluorescence emission (medium line, b) and FLN (thin line, a) spectra of yeast Zn cyt *c* in glycerol/water. Temperature: 10 K. Excitation for b: 415 nm (10 nm bandpass). Excitation for a: 17,740 cm^{-1}.

In Figure 3, absorption, emission and FLN spectra are shown for horse Zn cyt *c* in trehalose glass.

Details of the absorption and fluorescence vary between the two similar proteins: horse and yeast Zn cyt *c*. Since at low temperature, rearrangement of dipolar molecules around the excited state molecule cannot occur, the lack of coincidence between absorption and fluorescence cannot be due to a solvent relaxation process. The FLN spectra are considerably narrower than the conventional spectra, indicating that the sample is inhomogeneously broadened.

Multiple 0,0 Transitions

It was pointed out by Personov and coworkers [5] that in an inhomogeneously broadened sample a single frequency line can excite multiple bands. Using an energy

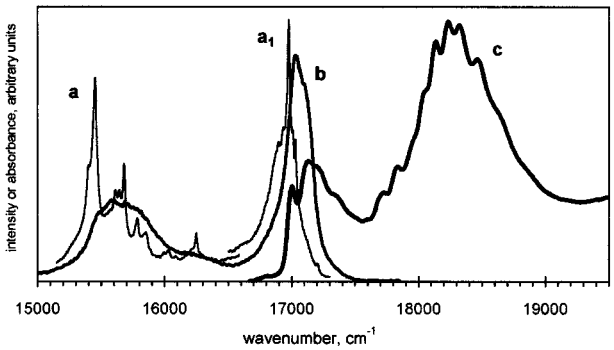

Fig. 1. Absorption (thick line, c), conventional fluorescence emission (medium line, b) and FLN (thin line, a) spectra of horse Zn cyt *c* in glycerol/water. Temperature: 10 K. Excitation for b: 420 nm (10 nm bandpass). Excitation for a_1: 17,940 and for a: 17,011 cm^{-1}.

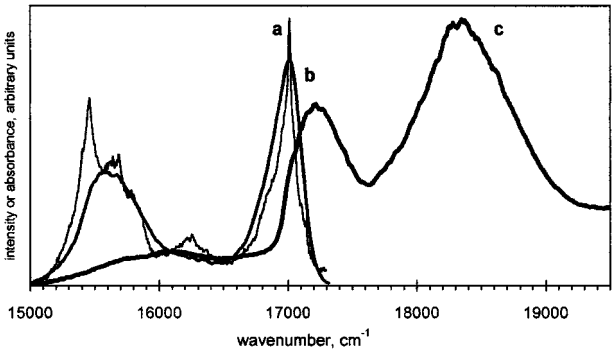

Fig. 3. Absorption (thick line, c), conventional fluorescence emission (medium line, b) and FLN (thin line, a) spectra of horse Zn cyt *c* in trehalose. Temperature: 10 K. Excitation for b: 420 nm (10 nm bandpass). Excitation for a: 17,752 cm^{-1}.

map, as previously described [11], we can get the distribution of the 0,0 transitions.

In Figure 4 we see an expanded region for horse, yeast Zn cyt *c* in glycerol/water (A and B) and horse Zn cyt *c* in trehalose (C). Several features are noticeable. First, sharp peaks, indicated by cross and asterisk, shift with the excitation frequency. These peaks, identified as 0,0 bands, are what are used to determine the IDF. The second is that there is a broad underlying band in all samples that remains approximately constant with excitation frequency.

Absorption, Emission and IDF of Horse and Yeast Zn cyt *c*

Figure 5 shows the expanded $Q(0,0)$ region, along with the data from the IDF. The conventional fluorescence spectrum does not show the fine detail of the IDF, and it is obvious that an estimation of the lowest transition using a conventional broad beam exciting light will give an error.

EFFECT OF INHOMOGENEOUS BROADENING ON THE EXCITATION PROCESS

Modeling the spectra for inhomogeneously broadened samples

Vibrational relaxation in porphyrins occurs mainly through intramolecular vibrational modes and occurs on the psec time scale. Because the excited state is long (~3 nsec) relative to reasonable estimates of vibronic relaxation, the emission occurs from the lowest vibrational level of the excited state (1,0) and the lorentzian linewidth is determined by the vibrational relaxation time. We consider what happens in the case of inhomogeneously broadened set of molecules.

The absorption characteristic of a single molecule embedded in a matrix at a certain vibronic level (site absorption function, SAF) can be described through a narrow Lorentzian function (zero phonon absorption/line or resonant absorption) and through a much wider phonon wing (a part of the absorbed energy that goes to the matrix, off resonant absorption)

$$\mathrm{SAF}(\varepsilon) = L(\varepsilon) + P(\varepsilon) = \frac{m}{1 + \left(\dfrac{\varepsilon - \varepsilon_0}{w}\right)^2} + P(\varepsilon) \qquad (1)$$

where m, ε_0 and w are the maximum value, the position and the width (half-width at half-maximum) of the lorentzian function, respectively. We use ε (energy) and wave number as synonyms. The functional form of the phonon wing, $P(\varepsilon)$ can be approximated by a gaussian and the contribution of the phonon wing into the unresolved background of the FLN emission spectrum is known. We want to point out that, beside the phonon wing excitation, the resonant absorption can give a contribution into the unresolved background, so we will use the resonant part ($L(\varepsilon)$) of the SAF only.

The possible positions are shown in Figure 6A1 for a few molecules and Figure 6B1 for a more realistic distribution. The latter shows so many lorentzian functions that they are individually not recognizable. We are using the term "site" to refer to molecules having the same SAF. The inhomogeneous distribution function (IDF = $\Delta N/\Delta\varepsilon$) gives the number of molecules in each site and the functional form is a gaussian (or gaussians) with a sigma around 10 to 100 cm^{-1} (e.g., 14 cm^{-1} in Figs. 6A2 and 6B2). The number of the different sites (N^*) is limited by the number of molecules. During the simulation we used the values of 21 (Fig. 6A) or 201 (Fig. 6B) or 20,001 (not shown) as N^*. The products of the SAFs and the corresponding values of the IDF give the series of weighted SAFs (Figs. 6A3 and 6B3).

$$(\mathrm{wSAF})_i = \left(\frac{\Delta N}{\Delta\varepsilon}\right)\Big|_{\varepsilon_i} \times (\mathrm{SAF})_i,\ i = 1,2,\ldots N^* \qquad (2)$$

The excitation selects from each wSAF with a certain probability. In the case of Dirac excitation (the function is different from 0 only at one value, ε_{laser}; Figs. 6A4 and 6B4), the probability that the ith site is excited is given by the value of the $(\mathrm{wSAF})_i$ at the ε_{laser}. These probabilities belong to each site and they give the site-weighted function (SWF).

$$(\mathrm{SWF})\big|_{\varepsilon_i} = (\mathrm{wSAF})_i\big|_{\varepsilon_{laser}} \qquad (3)$$

The SWF can have significant contribution from excitation in the lorentzian tails (Figs. 6A5 and 6B5). This is the most important observation of our simulation/model. If the excitation occurs into the edge of the IDF, one sharp maximum is at the excitation energy (high absorption probability of "one" molecule) and another broad band is close to, but not at, the maximum of the IDF (due to the low absorption probability of many molecules). When the excitation is at the high-frequency side, the mirror image will be obtained. In other words, the excitation into the lorentzian wings leads to excitation of molecules distributed toward the center of the inhomogeneous background and gives an apparent unresolved fluorescence background.

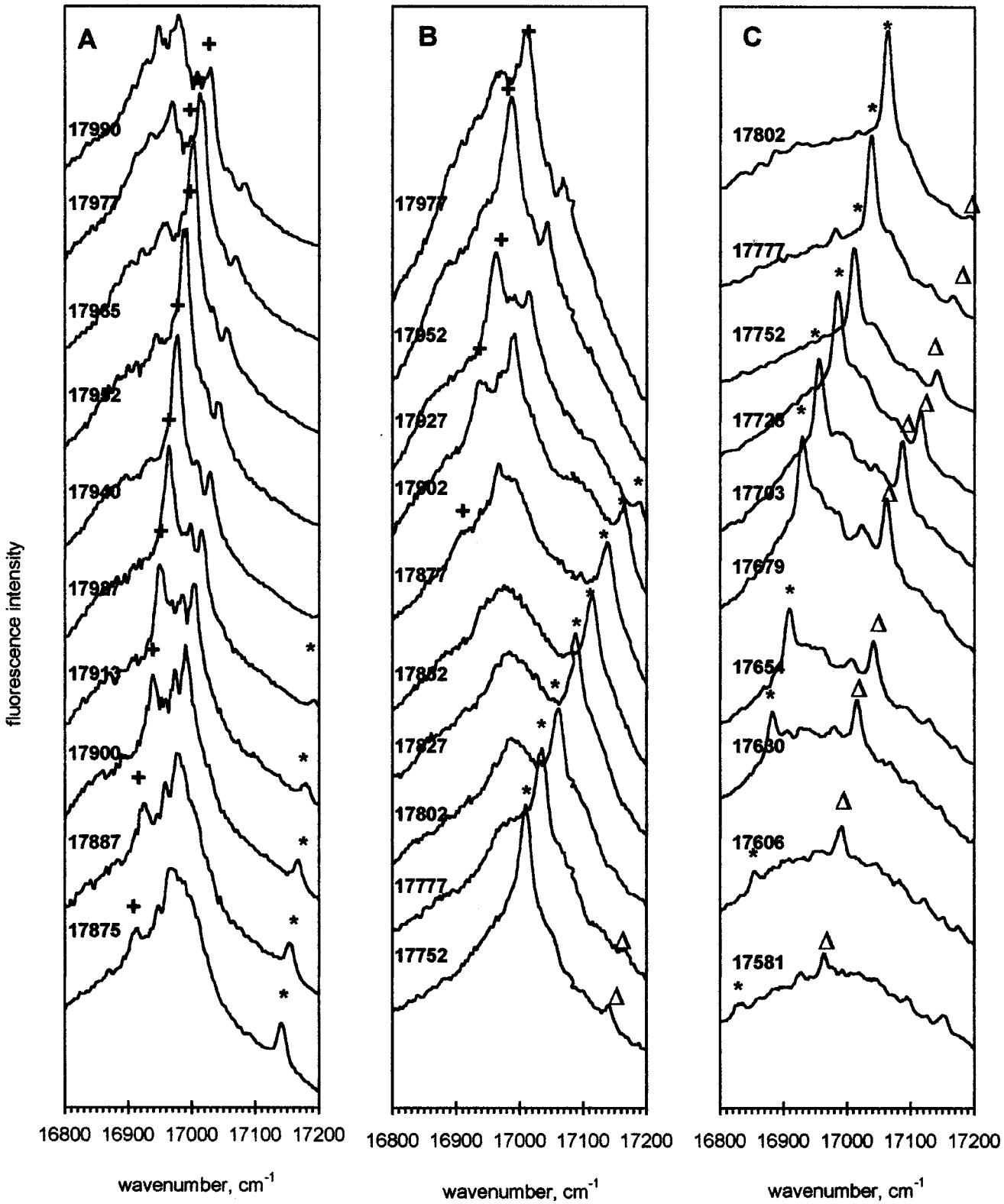

Fig. 4. FLN spectra in the *Q*(0,0) region as a function of excitation frequency. (A) Horse Zn cyt *c* in glycerol/water. (B) Yeast Zn cyt *c* in glycerol/water. (C) Horse cyt *c* in trehalose. Conditions are given in the legend of Fig. 2 and 3. Excitation frequencies in cm^{-1} noted on the Figure. Some ZPL (corresponding to excited state vibrational frequencies) are marked: * 740 cm^{-1}, triangle 616 cm^{-1}, + 964 cm^{-1}.

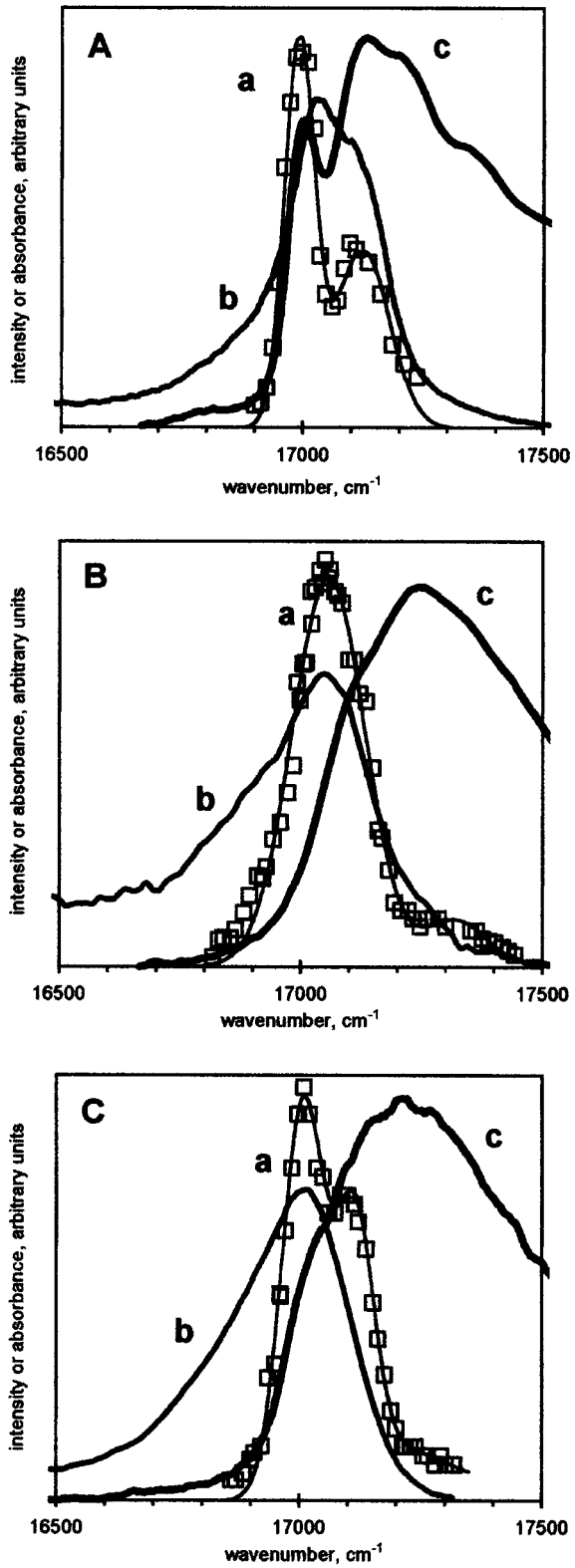

Fig. 5. (A) Absorption (c), emission (b) and IDF (a) of horse Zn cyt *c* in the *Q*(0,0) region in glycerol/water. (B) Absorption (c), emission (b) and IDF (a) of yeast Zn cyt *c* in the *Q*(0,0) region in glycerol/water. (C) Absorption (c), emission (b) and IDF (a) of horse Zn cyt *c* in the *Q*(0,0) region in trehalose

To get the contribution of each site in the fluorescence emission each site emission function must be multiplied by the corresponding value of the SWF (Figs. 6A6 and 6B6).

$$(\text{wSEF})_i = (\text{SWF})|_{\varepsilon_i} \times (\text{SEF})_i,\ i = 1, 2, \ldots, N^* \qquad (4)$$

The fluorescence emission spectrum for the 0,1 region is the sum of these weighted site emission functions (SEFs) (Figs. 6A7 and 6B7). The spectrum consists of two parts: zero phonon line (ZPL) and the zero phonon tail effect or zero phonon wing (ZPW). The position of the ZPL depends on the excitation wave number and the excited state vibrational energy: $\varepsilon_{zpl} = \varepsilon_{exc} - \varepsilon_{vibr}$. Figure 6 shows a simplified situation in which the $\varepsilon_{vibr} = 0$. The values of abscissa of Figures 6A6, 6B6, 6A7, and 6B7 must to be lowered by the frequency of the vibronic relaxation. The broad band is the consequence of the lorentzian tail excitation. The distinction between excitation into the peak of the lorentzian line (i.e., ZPL) and the tails can only definitely be seen in the cases of excitation into the edge of the IDF. The ratio of the intensities of ZPL and the broad band from the tail depends on the width of the IDF (FWHM in Fig. 6 is 33 cm^{-1}) and the width of the lorentzian. As noted above, excitations into the *Q*(0,0) band corresponds to an extremely narrow lorentzian width ($\sim 10^{-3}$ cm^{-1} for *Q*(0,0) excitation), but the excitations into the *Q*(0,1) band correspond to a lorentzian width of the order of 1 to 10 cm^{-1} (FWHM in Fig. 6 is 4 cm^{-1}).

SIMULATION RESULTS

Simulated Spectra

In Figure 7 we show a simulated spectrum. The parameters of the unimodal IDF are 17,100 and 33 cm^{-1} as maximum position and FWHM, respectively. On Figure 7A the excitation energy can be, for example, 18,010 cm^{-1} and the excited state vibrational energies are 950 cm^{-1} (peak position at 17,060 cm^{-1}) and 865 cm^{-1} (peak position at 17,145 cm^{-1}). These two ZPL lines are shifted according to the excitation energy as can be seen on Figures 7B and 7C (excitation energies 18,005 and 18,000 cm^{-1}, respectively). The number of different sites considered during the simulation was 20,001. The result is not very sensitive to the number of sites in the range being considered (density of sites), provided it is large enough.

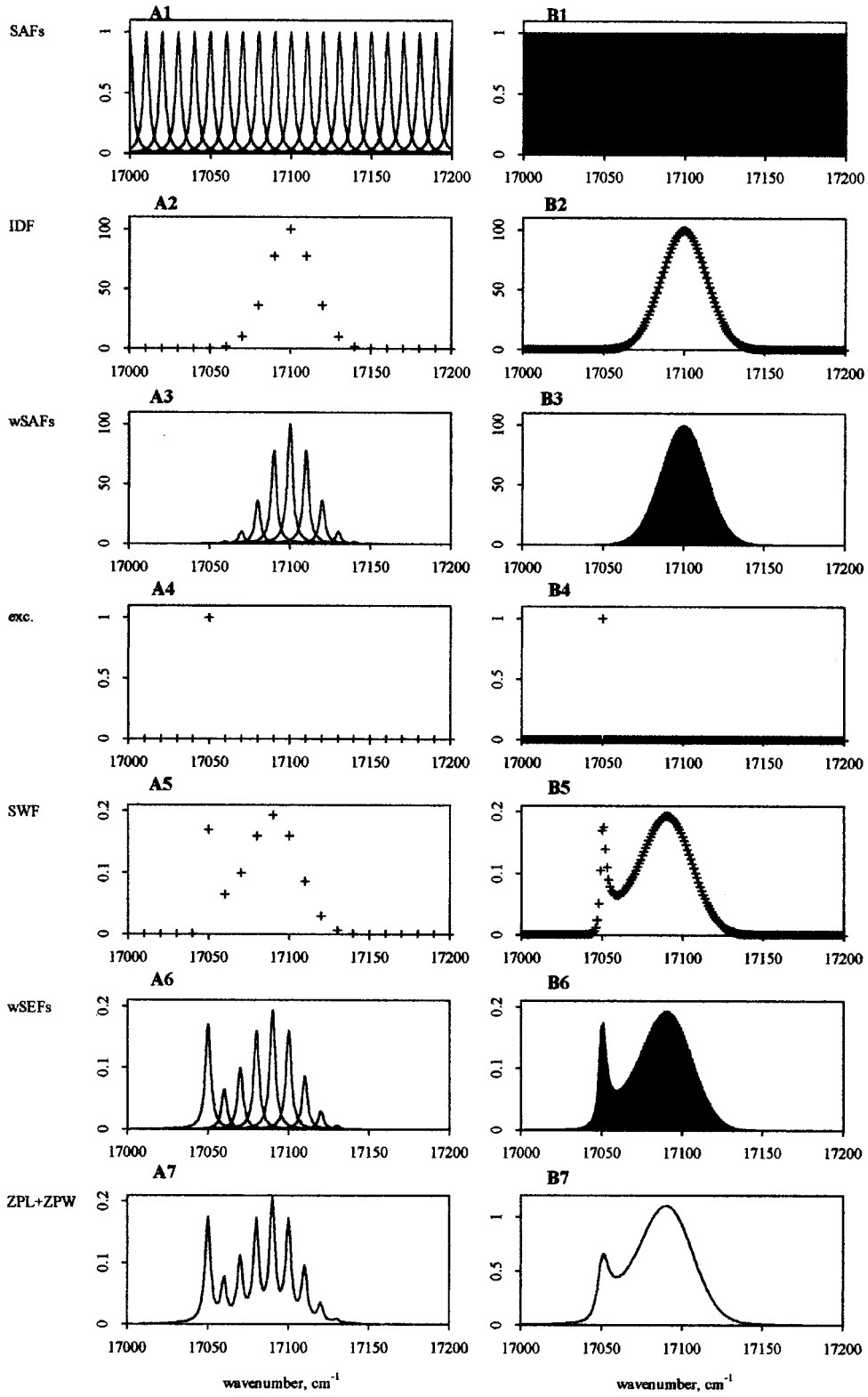

Fig. 6. Lorentz/gaussian function. Analysis procedure. Same procedure can be seen in two cases. (A) Number of sites: 21, (B) Number of sites: 201. First pair of panels: site absorption functions, second pair of panels: inhomogeneous distribution function, third pair of panels: weighted site absorption functions, fourth pair of panels: function of excitation; a Dirac function was used. Fifth pair of panels: site weight function, sixth pair of panels: weighted site emission function, seventh pair of panels: simulated fluorescence emission function (zero phonon excitations considered only: ZPL +ZPW). FWHM for lorentzian lines is 4 cm^{-1} and FWHM for gaussian distribution is 33 cm^{-1}.

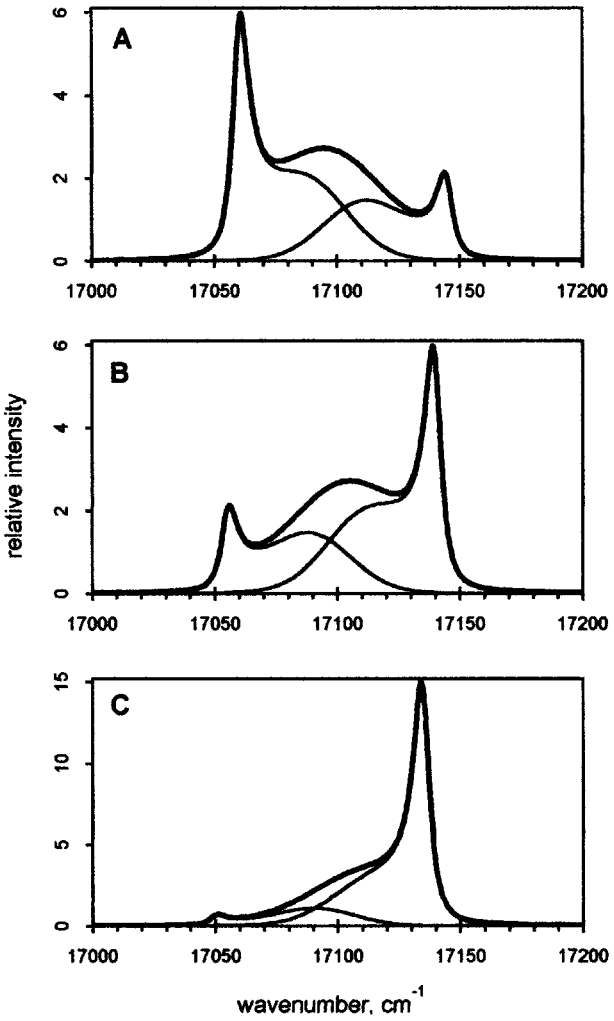

Fig. 7. Simulation of FLN spectra at different excitation energies. Maximum of IDF is at 17,100 cm^{-1} with a FWHM 33 cm^{-1}. FWHM for lorentzian lines is 4 cm^{-1}. Two hundred one sites are used over 200 cm^{-1} range. Excitation function is a Dirac delta. Excitation energies are: (A) $(x + 10)$ cm^{-1}, (B) $(x + 5)$ cm^{-1}, (C) x cm^{-1}, where x is an arbitrary value (e.g., $x = 18{,}000$ cm^{-1}). Thin line: ZPL + ZPW excitation of one vibrational level. Thick line: the sum of the subspectra.

In the simulated case 201 sites are large enough when we use Dirac delta excitation. We used 20,001 data points over a 200 cm^{-1} range to be able to use a narrow gaussian function for excitation. The simulated spectra very slightly depend on the shape of the excitation function if it is at least one order of magnitude smaller than the lorentzian line width, which characterizes the absorption and the vibrational relaxation processes. If this assumption is not true, there is a broadening of the ZPL (laser limited line width). The series of excitations qualitatively shows the similar behavior as the series of real spectra (Fig. 4).

CONCLUSIONS

We point out that both the uncertainty broadening and the closely lying transition energies for the population of the molecules in a glass affect the observed resolution of FLN.

The fluorescence spectra from porphyrin of Zn cyt *c* illustrate this. All the derivatives show inhomogeneously broadened fluorescence, as proved by obtaining resolution under the conditions given in Figures 1–3. The fast relaxation from the Q_y excited state to the Q_x excited state means that resolution is not seen when excitation is into the Q_y level. The energy gap between the Q_x and Q_y is smaller for the yeast protein, relative to the horse derivative. Even though the absorption spectra do not resolve the bands of Q_x and Q_y, the lower energy absorption band can be obtained from the IDF (Figs. 5A and 5B). In all cases in the FLN spectra there is a broad background (Fig. 4). This feature is accounted for by considering excitation into the tail portions of the lorentzian lines and the phonon wings (Fig. 7). The effect of inhomogeneous broadening on the IDF is shown when Figures 5A and 5C are compared. The trehalose sample shows a wider distribution and the existence of more than one population of species. The trehalose glass is formed at higher temperature than the sample in glycerol/water. Since the glass formation would trap large-amplitude fluctuations, it follows the sample would have a wider inhomogeneous distribution. We surmise that the lower resolution seen in the FLN spectra for the sample in trehalose (Fig. 3) relative to the sample in glycerol/water (Fig. 1) may be due in part to the wider inhomogeneous distribution and hence more excitation into the tail portion of the lorentzian lines.

In summary, the vibrational relaxation times and the inhomogeneous broadening observed for chromophores in proteins and glasses have a significant influence on whether FLN spectra will be obtained.

ACKNOWLEDGMENTS

This work was supported by National Institutes of Health grant PO1 GM48310, cooperative grants from the National Science Foundation International NT 98123221 and Hungarian Academy of Science 122/1998, and Hungarian Grant OTKA T32117. The FLN experiments were carried out in the laboratory of Prof. Judit Fidy, and we thank her for her support. The GCC (BeOS) version of the simulation was implemented by Ambrus Kaposi.

REFERENCES

1. L. Cordone, A. Cupane, M. Leone, and E. Vitrano (1986). Optical absorption spectra of deoxy-and oxyhemoglobin in the temperature range 300-20 K. Relation with protein dynamics *Biophys. Chem.* **24**, 259–275.
2. V. Srajer, K. T. Schomacker, and P. M. Champion (1986) Spectral Broadening in Biomolecules *Phys. Rev. Lett.* **57**, 1267–1270.
3. K. T. Schomacker and P. M. Champion (1986) Investigations of spectral broadening mechanisms in biomolecules: Cytochrome-c *J. Chem. Phys.* **84**, 5314–5325.
4. A. Cupane, M. Leone, E. Vitrano, and L. Cordone (1995) Low temperature optical absorption spectroscopy: an approach to the study of stereodynamic properties of hemeproteins *Eur. Biophys. J.* **23**, 385–398.
5. R. I. Personov and O. N. Korotaev (1969) The nature of multiplets in the quasiline spectra of organic molecules *Sov. Phys.-Doklady* **13**, 1033–1036.
6. H. S. Eom, S. C. Jeoung, D. Kim, J.-H. Ha, and Y.-R. Kim (1997) Ultrafast vibrational relaxation and ligand photodissociation/photoassociation processes of Nickel(II) porphyrins in the condensed phase *J. Phys. Chem. A.* **101**, 3661–3669.
7. S. Ye, C. Y. Shen, T. Cotton, and N. M. Kostic (1997) Characterization of Zinc-substituted cytochrome c by circular dichroism and resonance raman spectroscopic methods *J. Inorg. Biochem.* **65**, 219–226.
8. P. J. Angiolillo, J. S. Leigh, Jr., and J. M. Vanderkooi (1982) Resolved fluorescence emission spectra of iron free cytochrome c *Photochem. Photobiol.* **36**, 133–137.
9. H. Koloczek, J. Fidy, and J. M. Vanderkooi (1987) Fluorescence line-narrowing spectra of Zn cytochrome *c*. Temperature dependence *J. Chem. Phys.* **87**, 4388–4394.
10. V. Logovinsky, A. D. Kaposi, and J. M. Vanderkooi (1991) Fluorescence line narrowed spectra of Zn and metal-free cytochrome c *J. Fluorescence* **1**, 79–86.
11. A. D. Kaposi and J. M. Vanderkooi (1992) Vibronic energy map and excited state vibrational characteristics of magnesium myoglobin determined by energy-selective fluorescence *Proc. Natl. Acad. Sci. USA* **89**, 11371–11375.
12. V. Logovinsky, A. D. Kaposi, and J. M. Vanderkooi (1991) Native and denatured Zn cytochrome c studied by fluorescence line narrowing spectroscopy *Biochim. Biophys. Acta* **1161**, 149–160.
13. E. S. Manas, W. W. Wright, K. A. Sharp, J. Friedrich, and J. M. Vanderkooi (2000) The influence of protein environment on the low temperature electronic spectroscopy of Zn substituted cytochrome c *J. Phys. Chem. B* **104**, 6932–6941.
14. I. Rasnik, K. Sharp, J. A. Fee, and J. M. Vanderkooi (2001) Spectral analysis of cytochrome *c*: Effect of heme conformation, axial ligand, peripheral substituents and local electric fields *J. Phys. Chem. B* **105**, 282–286.
15. K. S. Reddy, P. J. Angiolillo, W. W. Wright, M. Laberge, and J. M. Vanderkooi (1996) Spectral splitting in the α $Q(0,0)$ absorption band of ferrous cytochrome *c* and other heme proteins *Biochemistry* **35**, 12820–12830.
16. D. S. Gottfried, E. S. Peterson, A. G. Sheikh, J. Wang, M. Yang, and J. M. Friedman (1996) Evidence for damped hemoglobin dynamics in a room temperature trehalose glass *J. Phys. Chem.* **100**, 12034–12042.
17. S. J. Hagen, J. Hofrichter, and W. A. Eaton (1995) Protein reaction kinetics in a room-temperature glass *Science* **269**, 959–962.
18. G. M. Sastry and N. Agmon (1997) Trehalose prevents myoglobin collapse and preserves its internal mobility *Biochemistry* **36**, 7097–7108.
19. J. M. Vanderkooi, F. Adar, and M. Erecinska (1976) Metallocytochromes c: Characterization of electronic absorption and emission spectra of Sn^{4+} and Zn^{2+} cytochromes c *Eur. J. Biochem.* **64**, 381–387.